LBL-15754
Preprint

Lawrence Berkeley Laboratory
UNIVERSITY OF CALIFORNIA

Materials & Molecular
Research Division

Submitted to IEEE Transactions on Magnetics

ELECTRON MICROSCOPY OF Mn-Al-C MAGNETS

J.S. Gau, R.K. Mishra, and G. Thomas

February 1983

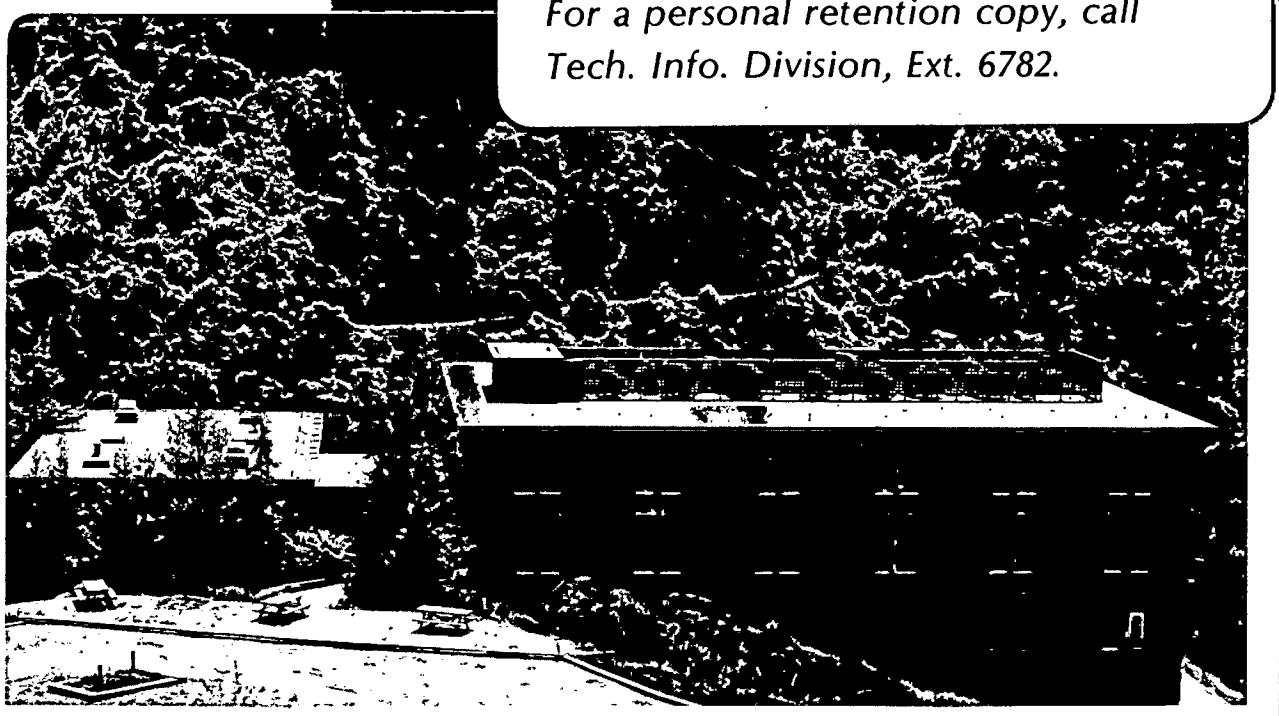

Prepared for the U.S. Department of Energy under Contract DE-AC03-76SF00098

ELECTRON MICROSCOPY OF Mn-Al-C MAGNETS

J. S. Gau, R. K. Mishra, and G. Thomas
Department of Materials Science and Mineral Engineering
and Materials and Molecular Research Division,
Lawrence Berkeley Laboratory, University of California,
Berkeley, California 94720

ABSTRACT

The microstructure of warm-extruded Mn-Al-C alloys with and without Ni addition have been characterized using scanning electron microscopy (SEM) and transmission electron microscopy (TEM) with x-ray microanalysis. The existence of finely dispersed Al_2O_3 particles in the extruded magnet is confirmed for the first time. Antiphase domain boundaries are not found, but, some grains are disordered. Other microstructural features such as twins and dislocations are characterized and the origin of these features are discussed. The role of Ni in improving the magnetic properties is attributed to its influence on (a) the deformation behavior of the material affecting the texture, (b) the magnetic-exchange interaction between Mn atoms and (c) the degree of ordering of the τ phase.

I. INTRODUCTION

New anisotropically hard Mn-Al-C magnets have become commercially available [1] and regained research interest because of two important developments, namely: (a) the addition of carbon to stabilize the metastable (τ) ferromagnetic phase, and (b) process techniques capable of producing these magnets efficiently are now available. These Mn-Al-C permanent magnets offer the following advantages: (1) easily available and comparatively cheap starting materials are needed, (2) the material has good machinability [2] and (3) it possesses reasonable magnetic properties [3].

The τ phase can be obtained from a high temperature disordered hexagonal ε phase in the Mn-Al system by controlled cooling or by quenching and annealing at temperatures between 400 and 600 °C [3]. The phase transformation involved has been well characterized by X-ray diffraction studies [4] on single crystal specimens and also by in-situ transmission electron microscopy studies [5]. The transformation sequences consist of an ordering reaction followed by a martensitic shear transformation to form the $L1_0$ face-centered tetragonal τ phase [5].

The temperature dependent magnetic properties such as anisotropy field H_A, coercivity H_C and saturation magnetization B_S have been measured by Rothwarf et al.

[6]. The reduced saturation magnetization follows the Bloch $T^{3/2}$ law. The theoretical $(BH)_{max}$ $(=B_s^2/4)$ yields a value of $12MGO_e$ at room temperature. The highest $(BH)_{max}$ obtained so far is $8.1MGO_e$ in the warm-extruded Mn-Al-C magnet containing a small amount of Ni [7].

The magnetic properties of crystallographically ordered ferromagnetic materials are strongly influenced by the structural (crystal) defects [8] which interact with the magnetic domain walls. In this investigation, transmission electron microscopy has been used to examine the defects and microstructural features in the warm-extruded magnets. These are correlated with the magnetic properties of the alloys. The effect of Ni on the microstructure and the magnetic properties is discussed.

II. EXPERIMENT

Two alloys of compositions: 69.7 wt% Mn, 29.8 wt% Al, 0.5 wt% C and 69.4 wt% Mn, 29.3 wt% Al, 0.5 wt% C, 0.8 wt% Ni were furnished by the Matshushita Electric Industrial Company of Japan. Details of the alloy preparation can be found in reference 2. The heat treatment consists of a quenching and aging process with subsequent extrusion at 600 ° C and a short annealing thereafter.

Thin foils for transmission electron microscopy (TEM) were prepared from thin slices cut from the extruded rods in the transverse direction. After cutting and careful grinding, electron transparent foils for TEM studies were prepared in a twin jet electropolishing apparatus with an electrolytic solution of percholic acid and methanol alcohol at room temperature. The foils were examined in a Philips EM 301 microscope operating at 100 kV. An analytical Philips EM 400 microscope was used for x-ray microanalysis as well as convergent beam diffraction experiments.

III. RESULTS AND INTERPRETATION

A typical scanning electron micrograph of the warm extruded magnet shows that the magnet consists of a fine grain material with small particles of a second phase dispersed in it (Fig. 1). These particles have been identified as Al_2O_3 by various techniques. The formation of Al_2O_3 particles and their morphology and distribution during extrusion are not discussed here and are subjects of a separate study. In this paper, a complete characterization of the matrix is presented.

The microstructural characteristics of the τ phase in the warm extruded magnets with and without Ni addition are summarized in Table 1.

Fig. 2 is a TEM micrograph taken from a Ni-containing specimen showing the typical microstructure. Some grains are highly dislocated and others are heavily twinned. Because of the fine grain size and high dislocation density, it has not been possible to determine the Burgers vectors of the dislocations by the $\underset{\sim}{g}.\underset{\sim}{b}$ contrast analysis. Fig. 2b is a convergent beam diffraction pattern taken from the grain with two variants of nearly edge-on twin bands. Indexing of the diffraction pattern and trace analysis of the twins on the micrograph show that the twins lie on { 111 } planes. Landuyt et al. [9] have reported similar microstructures in Mn-Al-C magnets. According to their interpretations, dynamic recovery occurs during the warm extrusion and high density of dislocation is due to the incompleteness of recrystallization during the short anneal after extrusion. Along this hypothesis, the thin twin lamellae are interpreted as recrystallization twins. This simple explanation is not a complete description of the twinning phenomena. We propose the following explanation according to which the twins are transformed twins and/or deformation twins.

During the ordering and subsequent martensitic shear to form the τ phase, twinning occurs to accommodate the localized stress associated with the volume and shape changes due to the formation of specific tetragonality axes. As the transformation pro-

ceeds, the long range stresses associated with different lamellae result in the formation of coarse twin bands as shown in Fig. 3. Fig. 3 is a typical dark field (DF) micrograph of the twin lamellae taken from a Ni-free specimen. The inset selected area diffraction pattern shows streaking along <111> direction that arises from the shape factor effect of the very thin twin bands. In addition to this transformation twinning, plasitc deformation during warm extrusion introduces deformation twinning. As is well known, plastic deformation can occur by slip and/or twinning both of which involve dislocation movement. It is to be noted that the deformation twinning in this $L1_0$ structure aids in developing texture by crystallographic shearing in a preferred direction with respect to the direction of maximum strain. Actually, Sakamoto et al. [10] have proposed a twinning model for the <001> texture in the anisotropic Mn-Al-C magnet. Among the twelve {111} <112> twinning systems, only four (one C axis for each {111} plane) which preserve the $L1_0$ ordered structure are responsible for the formation of texture.

There are many ways to induce magnetic anisotropy [11]. Extrusion is used as the means to produce the texture which coincides with the easy axis of magnetization. This preferred orientation in turn limits the final grain size. As already shown, the uniform fine grain size and higher twin density in the Ni containing

specimen imply that the addition of Ni helps in the deformation process to develop texture, i.e., a better easy axis alignment is achieved during extrusion. A further X-ray pole figure measurement is needed to confirm this point.

All efforts have failed to identify the existence of antiphase boundaries (APB's) in the ferromagnetic, ordered τ phase during this investigation. Curved APB's with fault vectors R = 1/2 <101> formed thermally by the growth and impingement of superlattice domains which are out of phase have been observed in the conventional non-extruded Mn-Al-C magnets[9]. The disappearance of APB's after extrusion has been postulated as due to the precipitation [3,9] of carbides at these boundaries.

The observation of APB's by TEM is non-trivial depending on (a) the phase angle, $\alpha = 2\pi \underset{\sim}{g} \cdot \underset{\sim}{R}$ where only certain superlattice reflections give rise to contrast, (b) the extinction distance and (c) the deviation from the exact Bragg angle. In the case of the $L1_0$ structure around the [001] pole as shown in Fig. 4, all APB's will be in contrast for any allowed superlattice reflection [12]. Careful bright field (BF) and dark field (DF) imaging and tilting experiments have failed to reveal any fault fringe contrast of APB's. It is to be noted that micrographs taken from foils with rough surface can exhibit contrast that may look like con-

trast from APB's, but, are actually thickness fringes and therefore need to be examined with caution. It is suggested that since the curved APB's are thermodynamically non-equilibrium defects, having a surface energy of the order of 120 erg/cm^2, [13] they migrate into the grain boundaries during extrusion and subsequent annealing. The small grain size and the large number of twins in the extruded magnets are all responsible for the absence of APB's.

X-ray microanalysis of the Ni-containing specimens in a Philips EM 400 microscope failed to reveal any partitioning of Ni in the grains except that occasionally a high Ni signal is detected in some grains as shown in Fig. 5. Due to the small grain size, attempts to determine the crystal sturcture by tilting experiments were not successful. We postulate that the severe deformation might cause segregation and further induce disordering. In fact, some grains are disordered in the extruded magnet with or without Ni addition as evidenced by convergent beam electron diffraction studies.

Lorentz microscopy [12] (defocus Fresenel technique) to image the magnetic domain walls, failed to image any domain walls in the Mn-Al-C magnet. The domain walls are believed to be present at the grain boundaries [9] where the diffraction contrast is strong enough to overwhelm any magnetic contrast. In the case of

Ni-containing specimens, domain walls could be occasionally observed within the grains.

IV. DISCUSSION

The τ phase with $L1_0$ structure is ferromagnetic due to the magnetic coupling between Mn atoms through indirect exchange interaction via the paramagnetic Al ions. As a result of the spin-orbit interaction, the material exhibits high magnetocrystalline anistropy ($K = 1 \times 10^7$ erg/cm^3) along the C-axis, which effectively impedes the magnetization reversal by rotation processes. However, the observed coercivity H_C is much less than the value $2K/M_S$, expected from a pure rotation model. This implies that other mechanisms such as domain nucleation and domain wall pinning contribute to the coercivity. The coercivity in the ferromagnetic Mn-Al-C magnet mainly arises from the pinning of domain walls at the grain boundaries and other crystal defects such as twins and dislocations. The role of the Al_2O_3 particles in impeding the domain wall motion also needs to be taken into account.

It has been well known [17] that the magnetic properties of Mn alloys are very dependent on the Mn-Mn distance. Furthermore, ferromagnetism is strongly influenced by short range order, (i.e., local atomic environment plays a crucial role in the magnetic pro-

perties). This has been realized in the Fe-Al (CsCl structure) ordered alloys through Mosshauser spectroscopy [16] studies that local magnetic moments associated with iron atoms in the non-stoichiometric $Fe_{1.1}Al_{0.9}$ and deformed $Fe_{1.0}Al_{1.0}$ alloys arise from the existence of iron-iron nearest neighbors. Similar arguments apply to non-stoichiometry in the binary Mn-Al and ternary Mn-Al-C magnets.

As discussed in Part III, the better magnetic properties in the Ni containing alloys can be attributed to the development of magnetic anisotropy as a result of a more favorable easy axis distribution. The addition of small amounts of Ni may promote the degree of ordering and affect the local atomic environments by substituting for Al atoms, Ni-Mn pairs will then interact ferromagnetically [18] contributing to the magnetic properties.

In conclusion, uniform alignment of the axis of easy magnetization, ultra fine grains and an increase in the degree of ordering are needed to achieve higher energy product and coercivity. Both alloy chemistry and processing techniques limit the development of these features.

V. CONCLUSION

The extruded Mn-Al-C magnet is fine grained with heavy twinning and a high density of dislocations and contains a dispersion of Al_2O_3. Although some grains are disordered, no anti-phase boundaries have been detected in the ordered $L1_o$ grains.

The effect of Ni addition on the structure-magnetic properties relation is established as follows: nickel helps in the development of magnetic anisotropy during the deformation process resulting in uniform fine grain and high density of twins. Atomistically, nickel atoms couple ferromagnetically with manganese atoms changing the local Mn atomic environment. All these account for the higher H_c and $(BH)_{max}$ values for the Ni containing Mn-Al-C magnet.

ACKNOWLEDGEMENT

This work was supported by the Director, Office of Energy Research, Office of Basic Energy Sciences, Materials Sciences Division of the U. S. Department of Energy under Contract No. DE-AC03-76SF00098. The Authors wish to thank the Matshushita Electric Industrial Company of Japan for supplying the material used in this study. Helpful discussions with Y. Sakamoto are acknowledged.

SUMMARY OF THE MICROSTRUCTURAL FEATURES

	Mn-Al-C	Mn-Al-C + 0.8 Ni
Grain Size	0.5-5um	0.2-1um
Texture	<001>	<001>
Twins	high density	higher density
Precipitates	Al_2O_3	Al_2O_3, NiS
Antiphase Boundaries	none	none
Magnetic Domain Walls	not observed	observed

REFERENCES

1. Wataru Owa, Teijro Mukakami, Yasuhiro Kondo, Tadao Otani, Shigeru Kojima and Y. Sakamoto, National Technical Report 26, 826-836, Oct. 1980.
2. T. Ohtani, N. Katop, S. Kojima, K. Komima, Y. Sakamoto, I. Konno, M. Tsukahara and T. Kubo, I. E. E. E. Trans. Mag. MAG-13, 1328-1330 (1977).
3. M. A. Bohlman, J. C. Koo and J. H. Wise, J. Appl. Phys. 52, 2542-2543 (1981).
4. S. Kojima, T. Ohtani, N. Kato, K. Kojima, Y. Sakamoto, I. Konno, M. Tsukahara and T. Kubo, AIP Conf. Proc. 24, 768-769 (1974).
5. J. J. Van den Broek, H. Donkersloot, G. Van Tendeloo and J. Van Landuyt, Acta Met. 27, 1497-1504 (1979).
6. R. Rothwarf, H. Leupold, J. T. Breslin, A. Tauber and D. I. Paul, J. Appl. Phys. 52, 2515-1516 (1981).
7. S. Kojima, K. Kojima, S. Mitani and T. Kubo, Synopsis of the 1978 Autumn Meeting of the Japanese Institute of Metals (1978).
8. J. P. Jakubovics , A. J. Lapworth and T. W. Jolly, J. Appl. Phys. 49, 2002-2006 (1978).
9. J. V. Landuyt, G. V. Tendeloo, J. J. v.d. Broek, H. Donkersloot and H. Zijlstra, I. E. E. E. Trans. Mag. Mag-14, 679-681 (1978).

10. Y. Sakamoto, S. Kojima, K. Kojima, T. Ohtani and T. Kubo, J. Appl. Phys. 50, 2355-2357 (1979).

11. B. D. Cullity, ntroduction to Magnetic Materials, Addison-Wesley Publishing Company, MA, 1979, Ch. 10.

12. P. B. Hirth, A. Howie, R. B. Nicholson, D. W. Pashley and M. J. Whelan, Electron Microscopy of Thin Crystals, Kriegar, New York, 1977, Ch. 15.

13. M. J. Marcinkowki, Electron Microscopy and Strength of Crystals,, G. Thomas and J. Washburn (eds.), Interscience Publishers, London, 1963, p. 431.

14. J. D. Livingston, J. Appl. Phys. 52, 2544 (1981).

15. J. P. Jakubovics and J. W. Jolly, Physica 86-88B, 1357-1359 (1977).

16. G. K. Wertheim and J. H. Wernick, Acta Met. 15, 297 (1967).

17. J. H. Wernick, Treatise on Solid State Chemistry, N. B. Hannay (ed.), Vol. 1, Plenum Press, New York, Ch. 4.

18. C. G. Shull and M. K. Wilkinson, Phys. Rev. 97, 304 (1955).

FIGURES

Fig. 1. (a,b) SEM micrographs showing the distribution and morphology of precipitates, (c) The corresponding Al mapping (d) The EDX spectrum taken from the precipitate (air melted samples).

Fig. 2. (a) A bright field TEM micrograph taken from a Ni-containing foil illustrates the typical microstructural features: dislocation, twins. (b) Convergent beam diffraction pattern taken from the grain containing two variants of edge-on twin bands. The corresponding index reveal twins lie on {111} planes (argon melting sample).

Fig. 3. A dark field TEM micrograph taken from a Ni free Mn-Al-C magnet shows the existence of thin and coarse twin lamellae. The selected area diffraction pattern shows streaking along 111 (air melting sample).

Fig. 4. A diffraction pattern of $L1_0$ ordered structure near 001 pole. The fundamental and super-lattice reflections are indexed.

Fig. 5. X-ray microanalysis spectra comparing the enriched Ni with the normal regions of the material (argon melted sample).

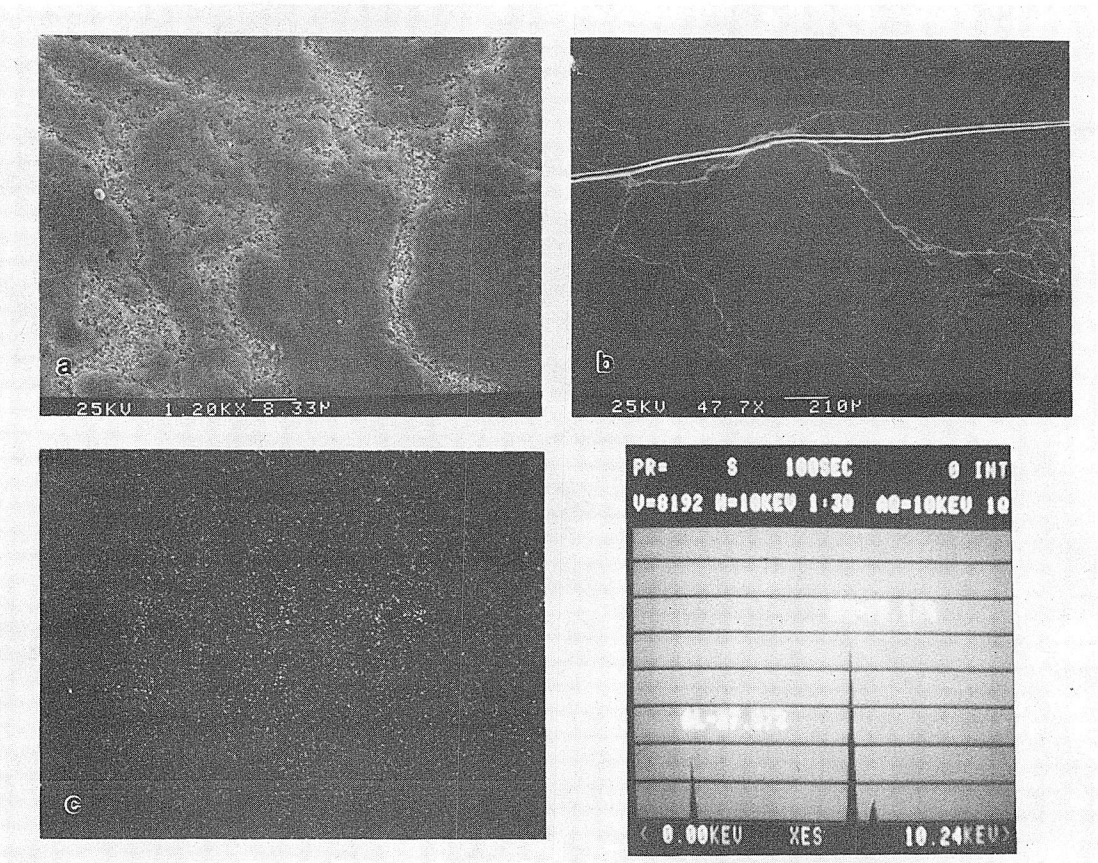

XBB 825-4357

Fig. 1

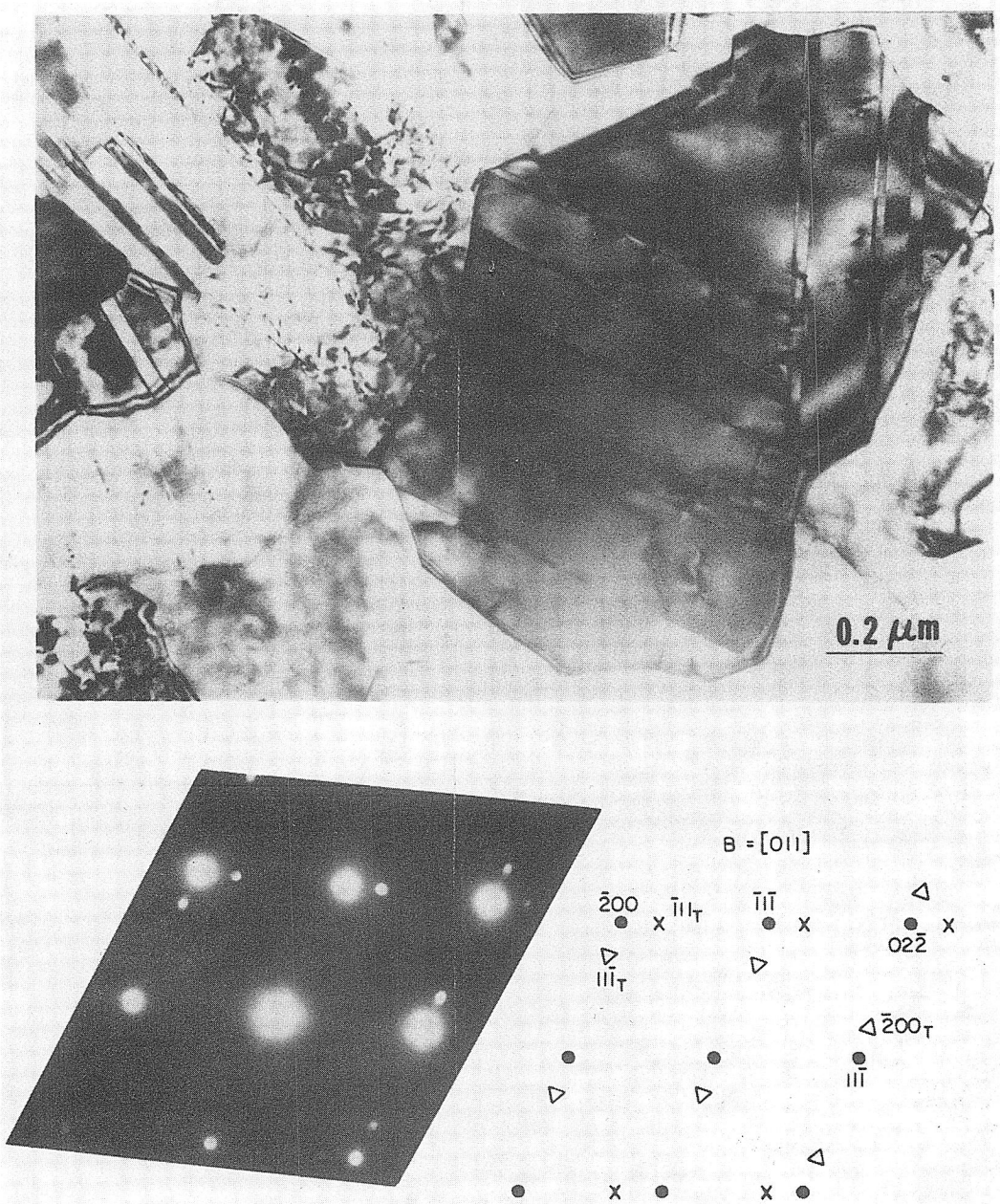

XBB 826-5177

Fig. 2

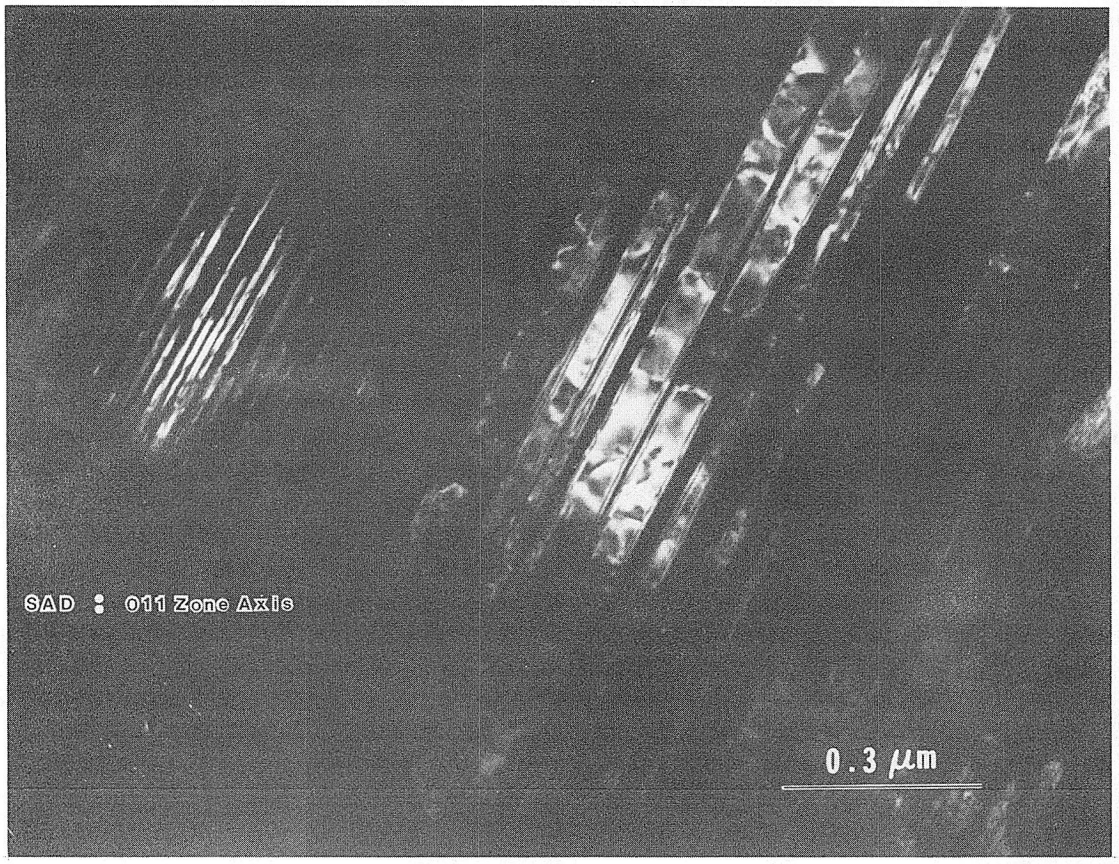

XBB 825-4208

Fig. 3

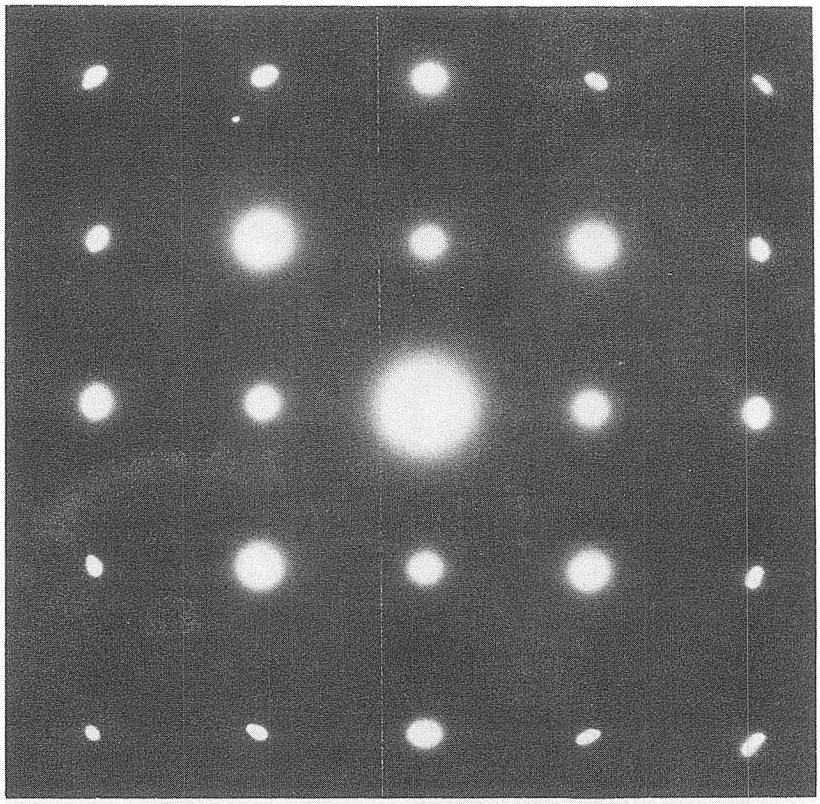

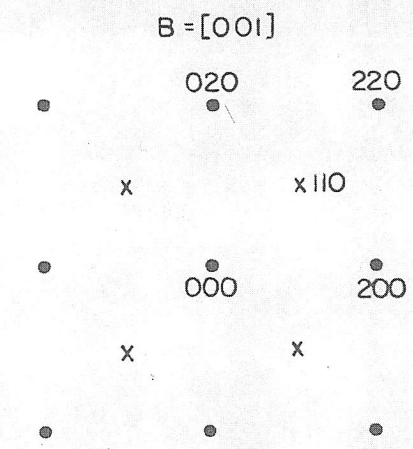

XBB 832-1317

Fig. 4

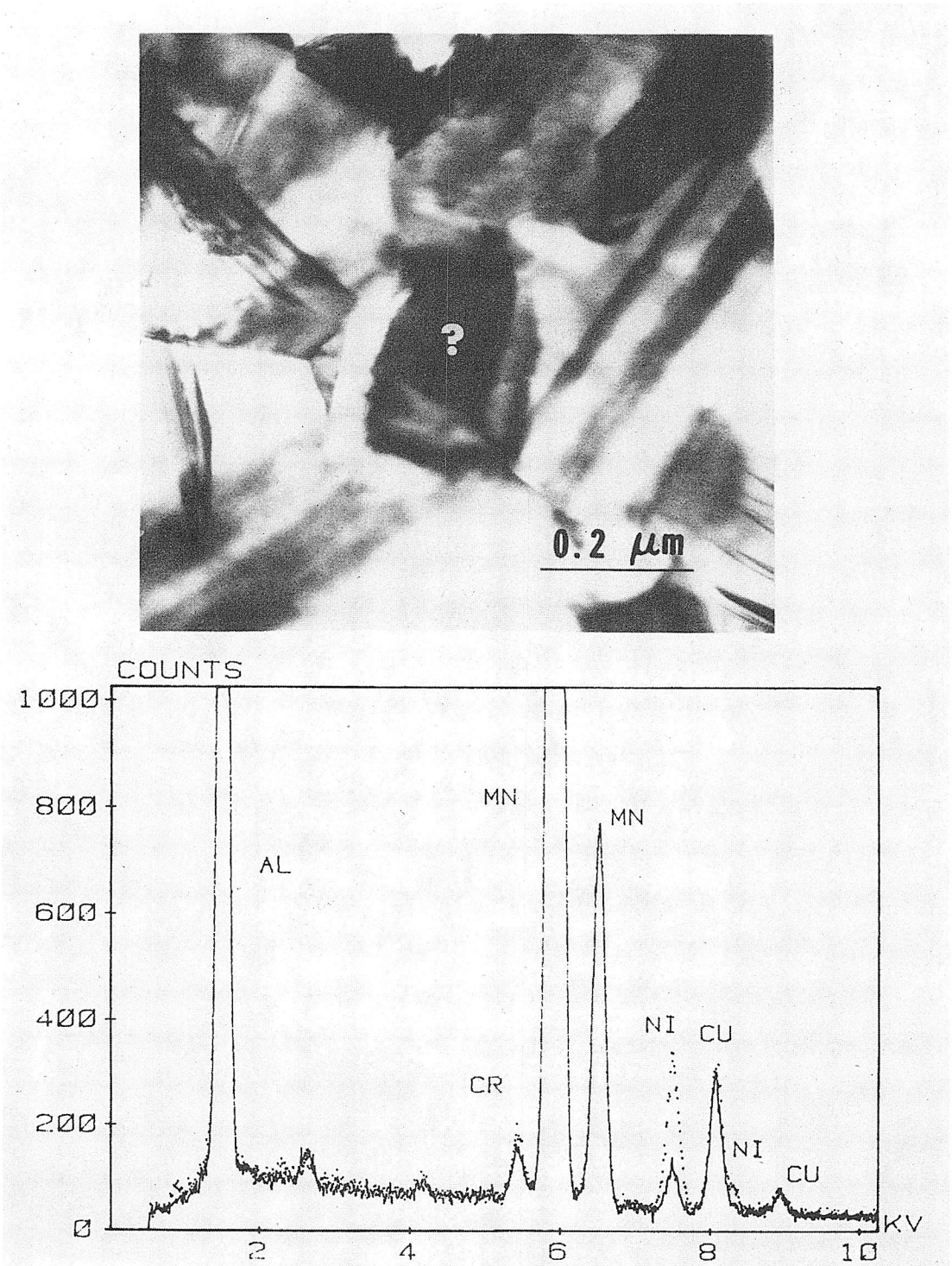

XBB 820-10354

Fig. 5

TECHNICAL INFORMATION DEPARTMENT
LAWRENCE BERKELEY LABORATORY
UNIVERSITY OF CALIFORNIA
BERKELEY, CALIFORNIA 94720